



# A multi-proxy assessment of terrace formation in the lower Trinity River valley, Texas

Hima J. Hassenruck-Gudipati<sup>1</sup>, Thaddeus Ellis<sup>1</sup>, Timothy A. Goudge<sup>1</sup>, David Mohrig<sup>1</sup>

<sup>1</sup>Department of Geosciences, Jackson School of Geosciences, The University of Texas at Austin, Austin, 78712, USA

*Correspondence to:* Hima J. Hassenruck-Gudipati (himahg@utexas.edu)

**Abstract.** A proposed null hypothesis for fluvial terrace formation is that internally generated or autogenic processes such as lateral migration and river-bend cutoff produce variabilities in channel incision that lead to the abandonment of floodplain segments as terraces. Alternatively, fluvial terraces have the potential to record past environmental changes from external forcings that include temporal changes in sea-level and hydroclimate. Terraces in the Trinity River valley have been previously characterized as Deweyville groups and interpreted to record episodic cut and fill during late Pleistocene sea-level variations. Our study uses high-resolution topography of a bare-earth digital elevation model derived from airborne lidar surveys along ~88 linear km of the modern river valley. We measure both differences in terrace elevations and widths of paleo-channels preserved on these terraces in order to have two independent constraints on terrace formation mechanisms. For 52 distinct terraces, we quantify whether there is a clustering of terrace elevations – expected for allogenic terrace formation tied to punctuated sea-level and/or hydroclimate change – by comparing variability in a chosen set of terrace elevations against variability associated with randomly selected terrace sets. Results show Deweyville groups record an initial valley floor abandoning driven by allogenic forcing, which transitions into autogenic forcing for the formation of younger terraces. For 79 paleo-channel segments preserved on these terraces, we connected observed changes in paleo-channel widths to estimates for river paleo-hydrology over time. Our measurements suggest the discharge of the Trinity River has changed systematically by a factor of ~2 during the late Pleistocene. Methods introduced here combine river-reach scale observations of terrace sets and paleohydrology with local observations of adjacent terrace-elevation change and paleo-channel bend number to show how interpretations of allogenic versus autogenic terrace formation can be evaluated within a single river system.

## 1 Introduction

Incised valleys commonly contain fluvial terraces, which exist at elevations above the modern floodplain. These terraces often host remnant river-channel segments whose widths, depths, bend amplitude and wavelength, and grain size preserve a signal of past river hydrology. Terrace formation requires net river incision that can be allogenic driven by tectonic uplift, sea-level fall, and/or modifications to water and sediment discharge via climate change (Hancock and Anderson, 2002; Pazzaglia, 2013; Bull, 1990). What is more controversial is the character of the trigger that leads to the relatively discrete transfer of a section of active floodplain or valley floor into an inactive terrace elevated above flood height. In particular, can



terraces formed by a punctuated sea-level fall or tectonic uplift be accurately separated from terraces formed by punctuated incisions connected with the autogenic processes of river channel migration and channel-bend cutoff? Here we use attributes of terraces and their preserved paleo-channels in the coastal Trinity River valley in order to evaluate the likelihood of allogenic versus autogenic processes driving terrace formation for previously established groups of Deweyville terraces (Blum et al., 1995; Bernard, 1950). Understanding how these terraces were most likely formed will help to constrain interpretations of the input signals for downstream coastal deposits, which are recognized to embed both allogenic and autogenic signals (Guerit et al., 2020).

Commonly invoked allogenic forcings connected with terrace formation are punctuated decreases in sediment-to-water flux that are assumed to embed a signal of regional climate and punctuated base-level fall controlled by sea-level fall or tectonic uplift, all of which can drive periods of increased vertical incision along an extended length of river channel (Bull, 1990; Pazzaglia, 2013; Pazzaglia and Gardner, 1993; Wegmann and Pazzaglia, 2002; Blum et al., 1995; Blum and Törnqvist, 2000; Hancock and Anderson, 2002; Rodriguez et al., 2005; Merritts et al., 1994; Daley and Cohen, 2018). These focused periods of downcutting are interpreted to produce a spatially extensive terrace, or set of terraces, that preserve a fraction of the active fluvial surface and its river channel at the time of the terrace-forming event (Bull, 1990; Molnar et al., 1994; Pazzaglia, 2013; Pazzaglia et al., 1998). This scenario provides a powerful opportunity to directly connect an observed distribution of terraces to a history of environmental or tectonic change. Within coastal river valleys, in particular, it is tempting to use the preserved terraces as a proxy for fluctuations in sea-level (Merritts et al., 1994; Blum et al., 1995; Blum and Törnqvist, 2000; Rodriguez et al., 2005).

It has also been shown that terraces can form by autogenic processes that drive spatially variable incision rates under conditions of persistent, allogenic forced base-level fall (Bull, 1990; Merritts et al., 1994; Muto and Steel, 2004; Strong and Paola, 2006; Finnegan and Dietrich, 2011; Limaye and Lamb, 2014). Autogenic terraces can be produced by channel narrowing (Muto and Steel, 2004; Strong and Paola, 2006) and river-bend cut off, both of which can increase bed incision rates via upstream propagating knickpoints (Finnegan and Dietrich, 2011). Additionally, numerical modelling has shown that autogenic terraces can form due to the intrinsic unsteadiness of lateral river migration (Limaye and Lamb, 2014, 2016).

Here we present a study of three previously classified sets of fluvial terraces composing the Deweyville Allogroup of the lower Trinity River valley (Young et al., 2012; Heinrich et al., 2020; Blum et al., 1995; Bernard, 1950) that have been interpreted as forming in response to punctuated allogenic forcing that includes Pleistocene sea-level fluctuations and climate-controlled changes in water to sediment flux (Blum et al., 1995; Rodriguez et al., 2005; Blum and Aslan, 2006; Blum et al., 2013; Anderson et al., 2016; Saucier and Fleetwood, 1970). Here we analyze whether these purported punctuated allogenic drivers can be distinguished from a null hypothesis that these terraces were formed by autogenic processes during long-term valley incision associated with persistent sea-level fall during the Last Glacial Period (from the end of the Eemian to the Last Glacial Maximum). To do this we implement a multi-proxy approach that (1) compares variability in elevations of terraces within an Allogroup against elevation variability for randomly selected terraces and (2) evaluates temporal changes in paleo-hydrology as defined by segments of paleo-channels preserved on terrace surfaces. Our analysis reveals that the upper set of



65 terraces indeed is most likely the product of punctuated allogenic change, while the lower set of terraces is most likely the product of autogenic processes, and the formational driver for the third, intermediate set of terraces is equivocal. This result documents how the study of terraces can be employed to substantially refine paleo environmental interpretations that are generated using these preserved fragments of paleo-landscapes.

## 2 Geological Setting

70 The Trinity River has the largest drainage basin contained entirely within the state of Texas, with an area of over 46,000 km<sup>2</sup>. It flows from northwest of Dallas, Texas, to Trinity Bay, where it empties into the Gulf of Mexico. Our study area is an ~88 linear-km stretch of the lowermost Trinity River valley from just north of Romayor, Texas, to just north of Wallisville, Texas (**Fig. 1**). Prone to flooding, the 2000 – 2020 hydrograph for the Trinity River has a median peak-annual discharge of 1679 m<sup>3</sup>/s at Romayor, TX (USGS 08066500) and 1484 m<sup>3</sup>/s at Liberty, TX (USGS 08067000) (National Water Information  
75 System data available on the World Wide Web (USGS Water Data for the Nation); National Water Information System data available on the World Wide Web (USGS Water Data for the Nation)).

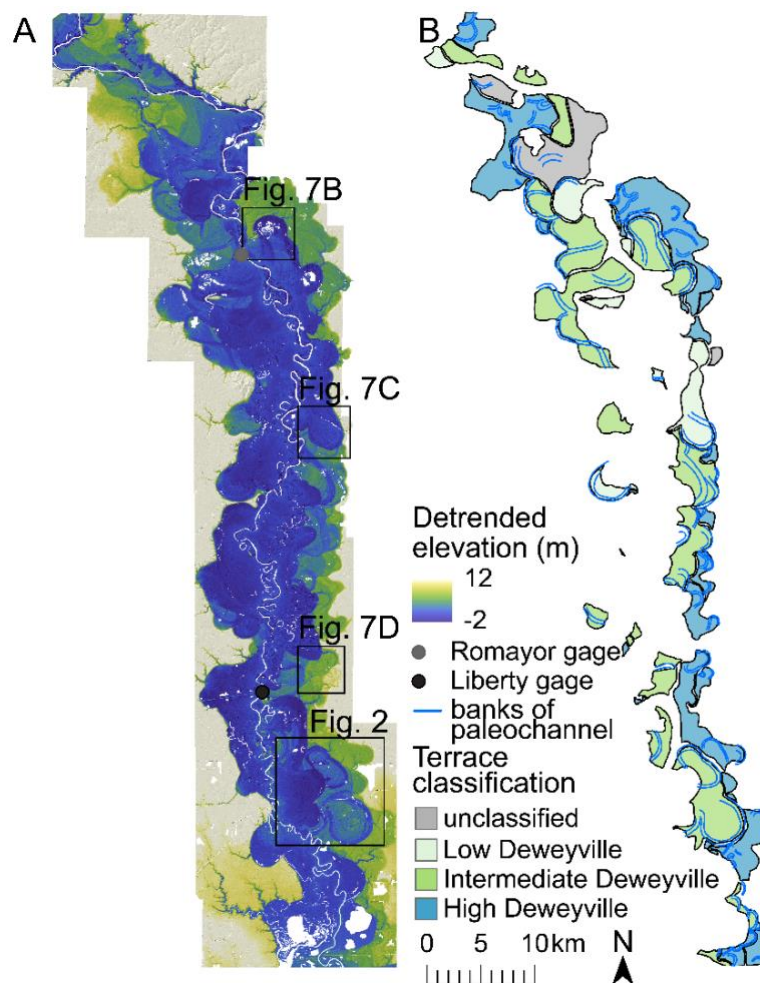
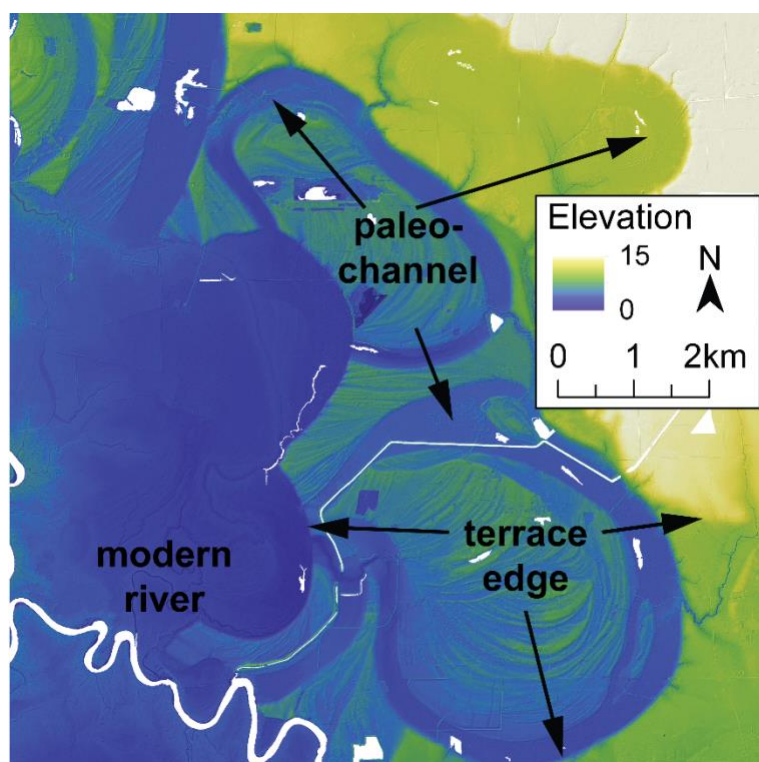


**Figure 1.** 2011 bare earth digital elevation model (DEM) from airborne lidar (A) with terrace and paleo-channel outlines (B) of the Trinity River, Texas, valley. (B) Terraces are preferentially distributed on the east of the valley. The black boxes mark the extent of Fig. 2 and 7B-D. USGS gage stations at Romayor and Liberty are marked in grey and black, respectively. The downstream extent of the data is ~10 linear km upstream of the river outlet into the Trinity Bay of the Galveston Bay.

The Trinity River has been subject to climate and sea-level variations throughout the Quaternary (Anderson et al., 2014; Simms et al., 2007; Galloway et al., 2000); however, the river catchment has never been glaciated and is interpreted to have maintained an approximately constant drainage area over this time (Hidy et al., 2014). The lower Trinity River valley is incised into the Beaumont and Lissie formations of Middle to Late Pleistocene age (Baker, 1995). Within the valley, Deweyville Allogroup terraces (Fig. 2) are post-Beaumont in age and formed prior to the Holocene. Age equivalent terraces with preserved segments of large paleo-channels are also found in alluvial valleys ranging from Mexico to South Carolina and are often classified as belonging to the Deweyville Allogroup. Traditionally, the formation of Deweyville terraces has been interpreted as the product of higher frequency Pleistocene sea-level cycles (Blum et al., 1995; Bernard, 1950; Anderson et al., 2016) with distinct episodic incision and subsequent valley deposition (Blum and Aslan, 2006; Blum et al., 2013). The history



of climatic variation, lack of glaciation, and superb preservation of late Pleistocene terraces make the lower Trinity River valley an ideal location to study terrace formation and to ask what processes these geomorphic features record.



95 **Figure 2. Morphological features of the Trinity River valley. Several terraces are preserved at different elevations with the black arrows marking the edges of the terraces. The labelled paleo-channel has a width that is ~2 times the modern river channel width.**

The Deweyville terraces have been divided into three Allogroups: high, intermediate, and low (Bernard, 1950; Blum et al., 1995; Young et al., 2012). Sea-level rise during the Holocene has induced valley-floor sedimentation that has partially buried the low-terrace Allogroup (Blum et al., 1995; Blum and Aslan, 2006). Age control for terraces in the lower Trinity River valley is limited to eight dates using optically stimulated luminescence (OSL) (Garvin, 2008). Based on these data, Garvin (2008) reports an OSL age of 35 - 31 ka for channel activity on high Deweyville terraces (N = 1), 34 - 23 ka for intermediate Deweyville terraces (N = 4), and 23 - 19 ka for low Deweyville terraces (N = 3). With only a single OSL date from the high Deweyville terraces, these features could be as old as 60-65 ka based on existing stratigraphic frameworks (Blum et al., 2013).

105 The Pleistocene sea-level curve for the Gulf of Mexico during the period of Deweyville terrace formation shows high-frequency variability superimposed on a longer-term net sea-level fall (Anderson et al., 2016; Simms et al., 2007). Between 35 and 19 ka, short-term rises and falls in sea-level are estimated to have been as large as 20 m and 60 m, respectively (Anderson et al., 2016). Deweyville Allogroups have been interpreted to represent three discrete sets of terraces formed during distinct oscillations in sea-level (Blum et al., 1995; Morton et al., 1996; Rodriguez et al., 2005; Anderson et al., 2016; Thomas and Anderson, 1994; Bernard, 1950). The three sets of terraces also have been interpreted as recording episodes of relative



110 sea-level stasis with extensive lateral migration of the river channel, separated by punctuated incision tied to accelerated sea-level fall (Blum and Aslan, 2006; Blum et al., 2013). The commonality between these two interpretations is an allogenic driver for terrace formation.

Paleo-channels have long been recognized to record past hydrologic conditions and associated climatic variations (Church, 2006; Knox, 1985). Terraces of the Trinity River valley preserve segments of abandoned river channels that range in  
 115 apparent widths and depths (**Fig. 2**). Previous researchers have interpreted increases in these paleo-channel widths and radii-of-curvature for paleo-channel bends as products of increased in river discharge and precipitation (Saucier and Fleetwood, 1970; Sylvia and Galloway, 2006; Church, 2006; Knox, 1985), and possible associated changes in vegetation and/or bank erodibility (Alford and Holmes, 1985; Saucier, 1994; Blum et al., 1995). The paleo-channel morphologies provide a record of external paleo environmental change in the lower Trinity River valley that is independent of any signal encapsulated in terrace  
 120 formation. Therefore, using both terrace elevations and paleo-channels, we have two geomorphic proxies to compare and contrast while assessing terrace formational processes among the Deweyville Allogroups.

### 3 Data and Methods

Our study used elevation data derived from four airborne lidar surveys collected for the Federal Emergency Management Agency (FEMA) and Texas' Strategic Mapping Program (StartMap) in 2011, 2017, and 2018 (FEMA, 2011;  
 125 StartMap, 2017a; StartMap, 2017b; StartMap, 2018). These four surveys were merged to produce a single bare earth digital elevation model (DEM) with 1 m<sup>2</sup> grid cells. The horizontal and vertical accuracies of the four original lidar point clouds are 0.6 m and 0.4 m, 0.25 m and 0.29 m, 0.20 m and 0.20 m, and 0.20 m and 0.20 m, respectively. All data were referenced to the NAD83 horizontal datum and the NAVD88 vertical datum.

Individual terraces and paleo-channels were manually mapped on the merged DEM using ArcGIS. A terrace was  
 130 defined as a genetically similar surface that is offset in elevation from its surrounding topography. Based on the maps of Blum et al. (1995), Garvin (2008), and Hidy et al. (2014), terraces were traced and classified as high, intermediate, or low Deweyville or marked as unclassified if the surface had not been previously identified. Elevations defining each terrace were extracted from the DEM using a 5 m grid resolution for a total of 164,520 measurements across all mapped terraces. From these elevations, the median value and interquartile range were found for each terrace. Since the Trinity River valley in the study  
 135 area trends N-S, this elevation data is plotted against median latitude for each terrace in **Fig. 3A**. A best-fit plane defining the modern valley floor was generated from a subsampled DEM with a 10 m grid resolution. This expression of the modern valley was used to generate detrended elevations for each terrace by subtracting it from the spatially corresponding median terrace elevations. The detrended median elevations and associated interquartile ranges for each terrace are presented in **Fig. 3B**. We then compared the distributions of detrended elevations for the terrace classifications. Each classified distribution, scaled to  
 140 its contribution to the overall number of detrended elevations is plotted in **Fig. 4**. The low, intermediate, and high Deweyville terraces have median values for detrended elevations of 0.03 m, 2.06 m, and 6.37 m. Even though their median values are





different, the detrended elevation distribution for the intermediate Deweyville terraces fully overlaps with that of the low Deweyville terraces (Fig. 4).

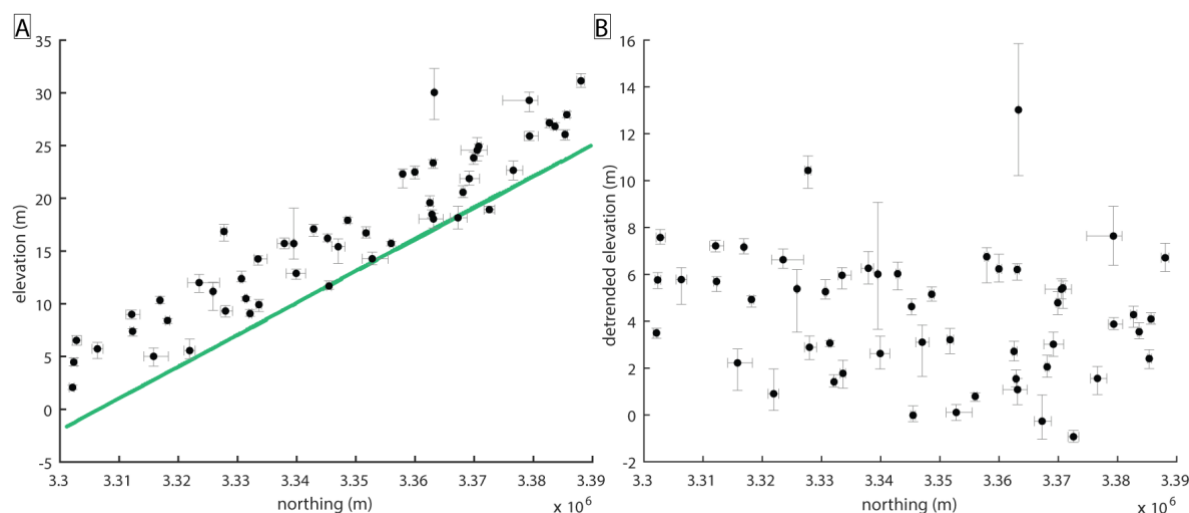


**Figure 3. Median terrace elevation (A) and detrended elevation (B) with interquartile range versus median terrace latitude (UTM) and interquartile range for the 52 terraces along the N-S trending valley. We cannot identify three distinct terrace classifications through visual inspection. The green line corresponds to the plane fitted to the 10m DEM of modern valley elevations.**

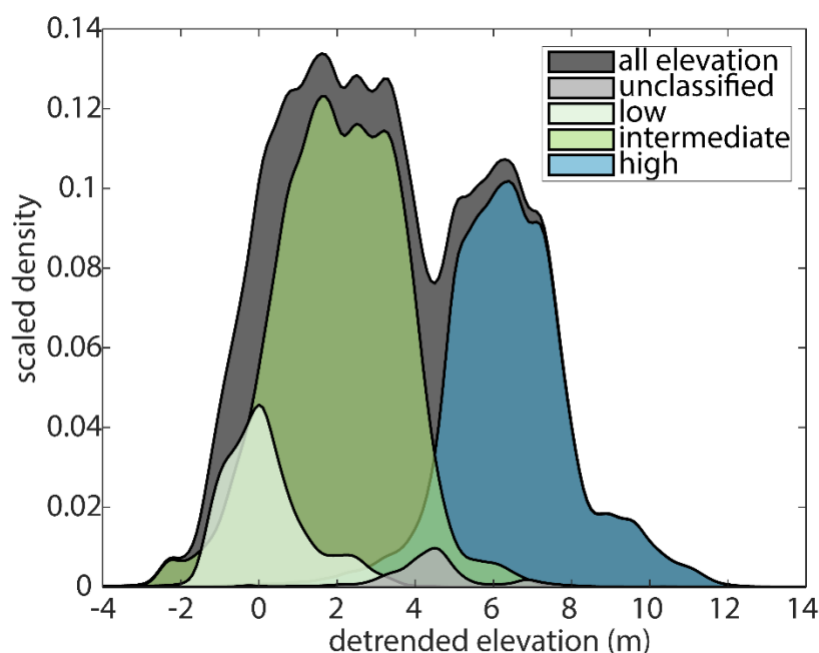


**Figure 4. Distributions of detrended elevations for terraces classified by Garvin (2008). Distributions were generated using a Gaussian kernel with bandwidth = 0.2 and scaled by the proportion of the total elevation points (164,520) present in each classification. There are 16,543, 84,784, 60,244, and 2960 points in the low, intermediate, high, and unclassified groupings, respectively. There is complete overlap between the detrended elevations of low and intermediate terraces. Terraces classified as high and intermediate have less overlap. The median detrended elevations for the low, intermediate, high, and unclassified Deweyville groupings are 0.3m, 2.05 m, 6.3 m, and 4.41 m.**



### 3.1 Testing Terrace Formation using Elevation Data

Following the proposal of Limaye and Lamb (2016), our null hypothesis for terrace formation is that incision driven by autogenic processes dominates terrace development. Only after formational mechanisms internal to the system have been considered and rejected, should we consider temporal variation in allogenic forcing as governing terrace formation. Our method for testing the null hypothesis acts to separate the regional signal of an allogenic driver from local terrace production by autogenic processes. It is based on the observation that allogenic terraces are regionally and synchronously isolated along the entire valley length and thus approximately preserve the valley paleo slope (Bull, 1990; Pazzaglia et al., 1998). It follows that a group of contemporaneous allogenic terraces should preserve lower variability in elevations about a best-fit plane estimating paleo slope than groupings of randomly selected terraces. Conversely, groupings of locally produced, autogenic terraces are not expected to be distinguishable from randomly selected terraces.

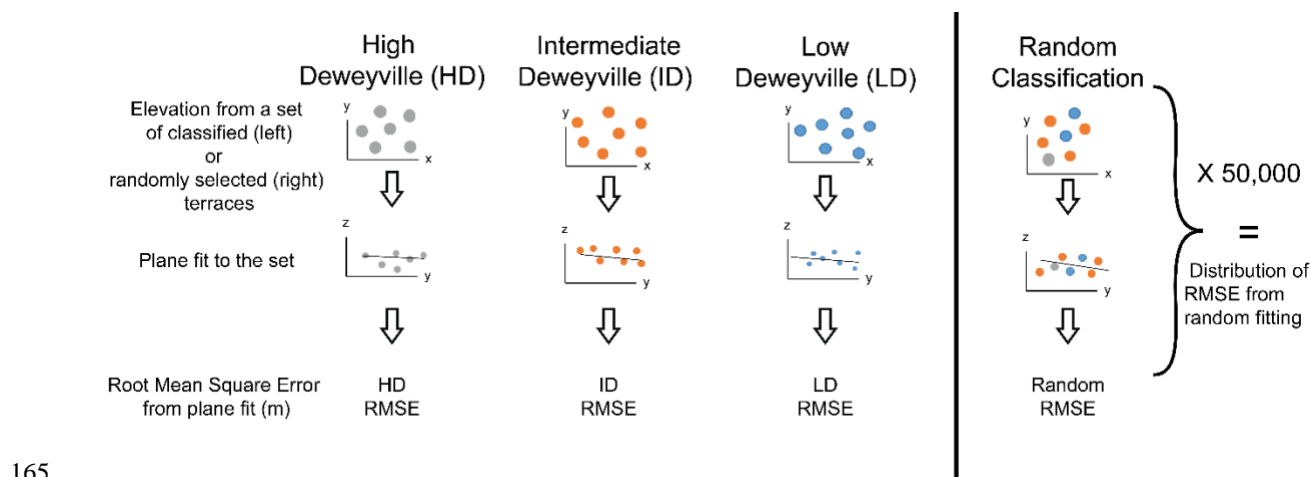


**Figure 5. Method to determine if classifications assigned to terraces represent distinct terrace groups. A plane was first fit to elevations extracted from the classified terrace groups in Garvin (2008) at a 5 m grid resolution. We then fit planes to three randomly grouped sets of terraces using the same elevation data, iterating 50,000 times, for a total of 150,000 fits (right of the black line). The root mean square error (RMSE) of the plane fit from each of the previously classified terrace groups was compared to the distribution of RMSE of the randomly grouped terraces (Fig. 6).**

We began our hypothesis testing by determining the best-fit plane to all of the elevation points (x, y, z) for terraces classified into the three Deweyville groups by Blum et al. (1995) and Garvin (2008) using a linear least-squares method. A planar surface was chosen for this analysis because the modern river-surface and valley profiles are linear in our area of study (Fig. 3A). The goodness of fit for these three planes to their associated terrace data was captured by the root-mean-square error (RMSE), which provides a measure of average variability of actual terrace elevations about the best-fit plane (Fig. 5). The next step was to compare the properties of these fitted planes against planes fitted to terraces randomly drawn from the overall population. The randomly assigned terraces were put into one of three groups that had the same number of elements as the





classified high (n= 22), middle (n=19), and low (n=8) Deweyville terraces. Best-fit planes were calculated and their RMSE fits were recorded. This process of randomly assigning terraces into three groups was then repeated 50,000 times in order to  
 180 derive a large dataset of elevation variability characterizing randomly grouped terraces (**Fig. 6**).

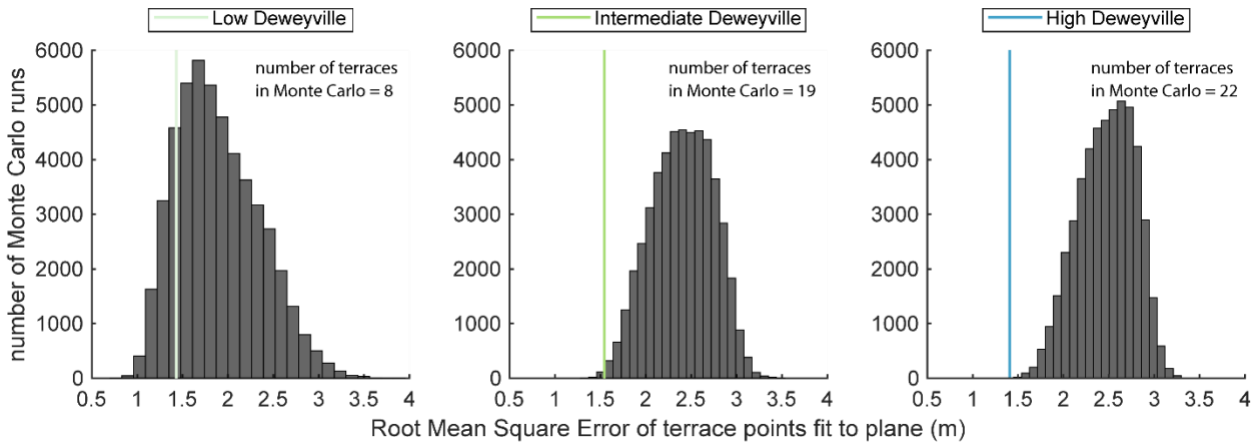


**Figure 6.** Root mean square error (RMSE) of a plane fitted to elevation points of terraces previously classified as high Deweyville, intermediate Deweyville, and low Deweyville in the Trinity River valley compared to a distribution of RMSE from 150,000 randomly grouped terraces. All of the Deweyville classifications fall within the distribution with the high Deweyville classification being the  
 185 closest to falling outside of the distribution, ~3.4 standard deviations away from the random terraces RMSE distribution mean of 2.47 m (22 terrace groupings). The low and intermediate Deweyville classification are ~1.0 and ~2.5 standard deviations away from the RMSE distribution mean of 1.89 m and 2.40 m for 8 and 19 terrace groupings, respectively.

### 3.2 Evaluating Terrace Formation using Paleo-Channel Analysis

Change in the discharge of the Trinity River during the late Pleistocene was estimated using segments of paleo-  
 190 channels preserved on terrace surfaces. Mean bankfull width ( $B_{bf}$ ) for each paleo-channel mapped on the bare-earth DEM (**Fig. 1B**) was calculated from measurements extracted at 10 m intervals along each paleo-centerline (**Fig. 7**). Representative sidewall slopes (rise/run) for these paleo-channels range between 0.02 and 0.26 (**Fig. 7A**). These paleo-sidewall slopes fall within the range of modern sidewall slopes measured for the Trinity River in the study area by Smith and Mohrig, (2017, their Fig. 4). Therefore, we confidently use the paleo-channel widths extracted from the DEM without any correction to the widths  
 195 associated with relaxation of the paleo-topography over time. These data were used to estimate a formative, bankfull discharge ( $Q_{bf}$ ) following the hydraulic geometry relationship developed by Wilkerson and Parker, (2011) :

$$\frac{B_{bf} g^{\frac{1}{5}}}{Q_{bf}^{\frac{2}{5}}} = 0.0398 * \left( \frac{D_{50} * \sqrt{R * g * D_{50}}}{\nu} \right)^{0.494 \pm 0.14} * \left( \frac{Q_{bf}}{D_{50}^2 \sqrt{g * D_{50}}} \right)^{0.269 \pm 0.031}, \quad (1)$$

where  $\nu$  is the kinematic viscosity of water,  $R$  is the specific gravity of the sediment ( $R = \frac{\rho_s - \rho}{\rho}$ ),  $\rho_s$  is sediment density,  $\rho$  is water density,  $g$  is gravitational acceleration, and  $D_{50}$  is the median grain size of transported bed material. We used a value of  
 200 2650 kg/m<sup>3</sup> for  $\rho_s$  and a range of paleo-channel grain sizes taken from Garvin (2008), who sampled both the lower and upper portions of bar deposits within preserved channel fills (**Table 1**). The uncertainty in estimated discharge was quantified for each paleo-channel using Monte Carlo simulation. For each run of the simulation, we sampled from: (1) normal distributions



with the reported means and standard deviations for each exponent in **Eq. 1**; (2) a normal distribution for channel width using its measured mean and standard deviation; and (3) a uniform distribution of grain sizes constrained by measurements from each classified terrace set (**Table 1**). This Monte Carlo simulation was run 50,000 times for each paleo-channel. Paleo-discharge estimates derived for the 79 channel segments preserved on terrace surfaces are plotted as a function of median detrended terrace elevation in **Fig. 8**.

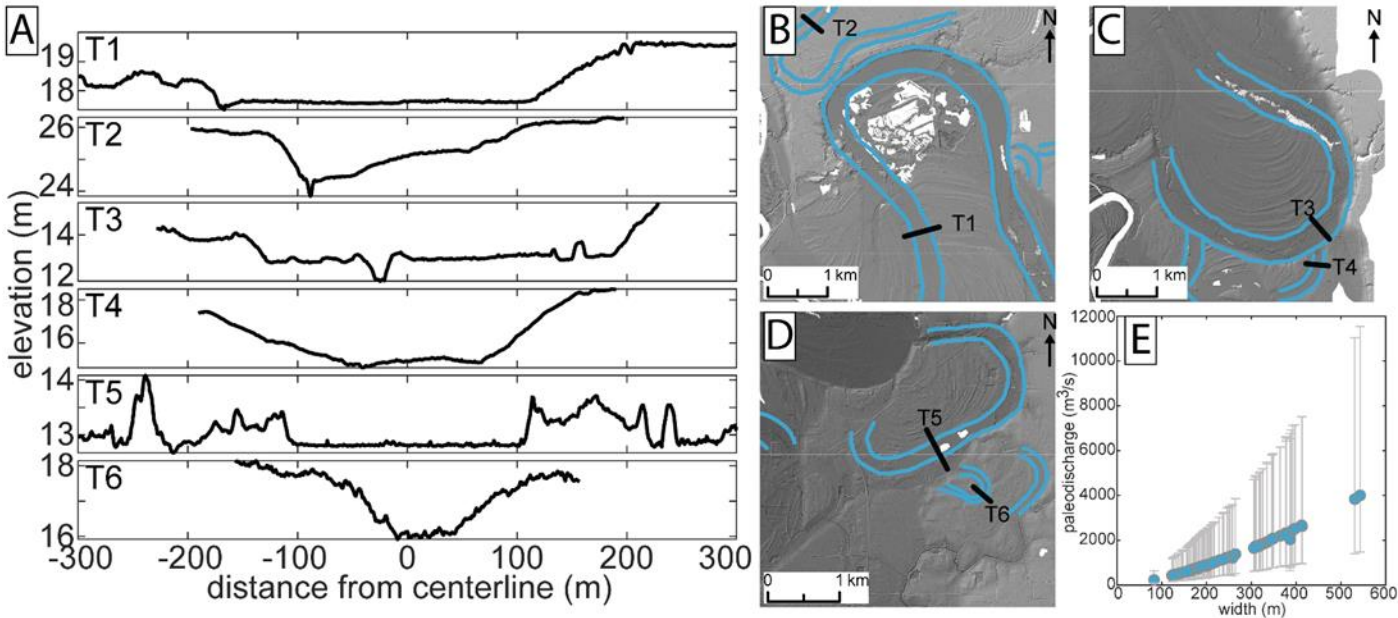


**Figure 7: Paleo-channel widths and paleo-discharge estimates. (A) Elevation transects for six paleo-channels (T1-T6). Transects are taken from locations indicated in (B)-(D) with mapped paleo-channels outlined in blue. (E) Paleo-discharge estimates for the Trinity River are plotted as a function of their width. Each paleo-discharge was calculate using preserved channel width measurements and the discharge-width relationship from Wilkerson and Parker (2011) (Eq. 1). Error bars represent the first and third quartile of paleo-channel discharge estimates and terrace elevations above the modern valley.**

Garvin (2008) Terrace classification	Upper bar deposit lower range (mm)	Upper bar deposit upper range (mm)	Lower bar deposit lower range (mm)	Lower bar deposit upper range (mm)	Average grain size (mm)
Low Deweyville	0.25	1.00	0.25	4.00	0.71
Middle Deweyville	0.125	1.00	0.50	2.00	0.59
High Deweyville	0.125	2.00	0.25	2.00	0.59

**Table 1: Grain size of terrace deposits from Garvin (2008), used for discharge calculations. The average grain size was calculated using the phi (logarithmic) scale.**

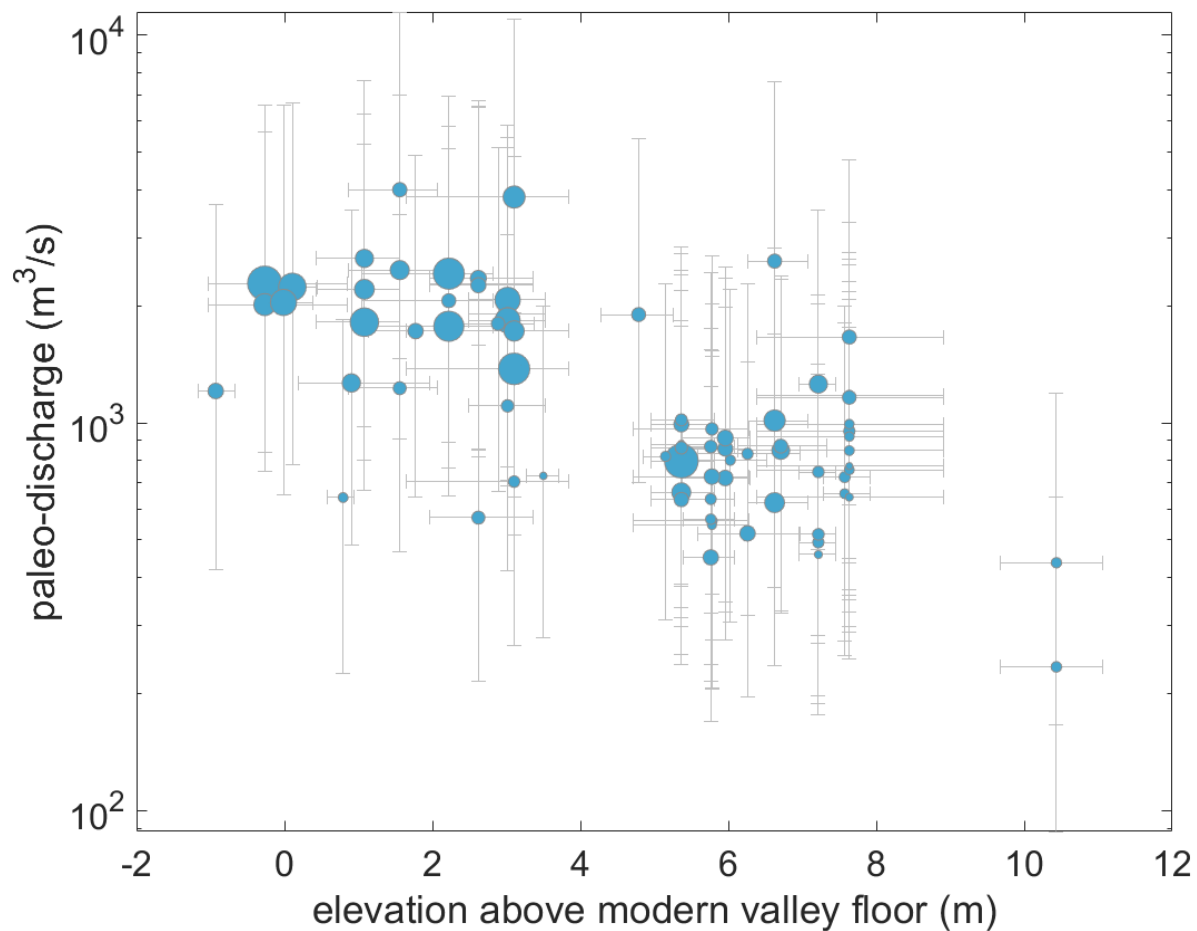


**Figure 8.** Paleo-discharge estimates for the Trinity River plotted as a function of their associated detrended terrace elevations. Elevations afford a crude stratigraphy for the discharges with the highest relative elevations representing older channels and lowest elevations representing younger channels. Each paleo-discharge was calculated using preserved channel width measurements and the discharge-width relationship from Wilkerson and Parker (2011) (Eq. 1). Error bars represent the first and third quartile of paleo-channel discharge estimates and terrace elevations above the modern valley. The symbol size for each discharge estimate was scaled to the preserved length for each paleo-channel, with larger symbols equated to longer segments.

Accuracy of the Wilkerson and Parker (2011) relationship for the Trinity River system was tested by calculating a  $Q_{bf}$  value for the modern river channel and comparing it against the bankfull discharge logged at the USGS gage 08067000 at Liberty, Texas. The calculated bankfull discharge was estimated using the measured bankfull width of 170 m from the DEM at the gage site. The median particle size of bed material at Liberty has been measured at 200 $\mu$ m by the Trinity River Authority of Texas (Trinity River Authority of Texas, 2017). All other variables in **Eq. 1** were kept constant between the modern river and paleo-channels, yielding an estimate for the modern bankfull discharge of 830 m<sup>3</sup>/s. The reported residual standard error associated with the bankfull discharge **Eq. 1** (Wilkerson and Parker, 2011) was then used to approximate the error associated



230 with this modern calculated bankfull discharge. The lower and upper standard error define a possible range between 340 and  
 2030 m<sup>3</sup>/s. These discharges estimated with **Eq. 1** favorably compare with the measured discharge found using the rating curve  
 for the USGS Liberty gage station ([https://waterdata.usgs.gov/nwisweb/get\\_ratings?file\\_type=exsa&site\\_no=08067000](https://waterdata.usgs.gov/nwisweb/get_ratings?file_type=exsa&site_no=08067000)) and  
 bank-line elevations for the swath of channel extending 300 m both upstream and downstream of the gage. The mean and  
 standard deviation of bank elevations for this swath was 7.68m and 0.34m, yielding a mean bankfull discharge of 1017 m<sup>3</sup>/s  
 235 and discharges of 887 m<sup>3</sup>/s and 1243 m<sup>3</sup>/s corresponding to stages  $\pm 1$  standard deviation in bank elevation.

### 3.3 Mixing Models and Bend Cutoff Analyses

To further test the statistical groupings within our terrace and paleo-channel data, a mixing model was used to generate  
 Gaussian mixture distributions that were fitted to both the 164,520 detrended terrace elevation points and the median discharges  
 estimated for the 79 paleo-channel segments (**Fig. 9**). The Akaike Information Criterion (AIC) and Bayesian Information  
 240 Criterion (BIC) were applied to both mixing models in order to optimize the number of components used to represent each  
 distribution (**Fig. 9C, 9D**). Two and three components were selected for the distributions of detrended elevation points and  
 median paleo-channel discharges, respectively (**Fig. 9A, 9B**). The mean and standard deviation of the detrended elevation  
 components are  $5.6 \pm 4.18$  m and  $1.32 \pm 2.19$  m with mixing proportions of 0.51 and 0.49, respectively. Similarly, the mean  
 and standard deviation for the three Gaussian distributions describing paleo-discharges are  $795 \pm 80$  m<sup>3</sup>/s,  $2083 \pm 139$  m<sup>3</sup>/s,  
 245 and  $4013 \pm 21$  m<sup>3</sup>/s with mixing proportions of 0.68, 0.30, and 0.02, respectively.

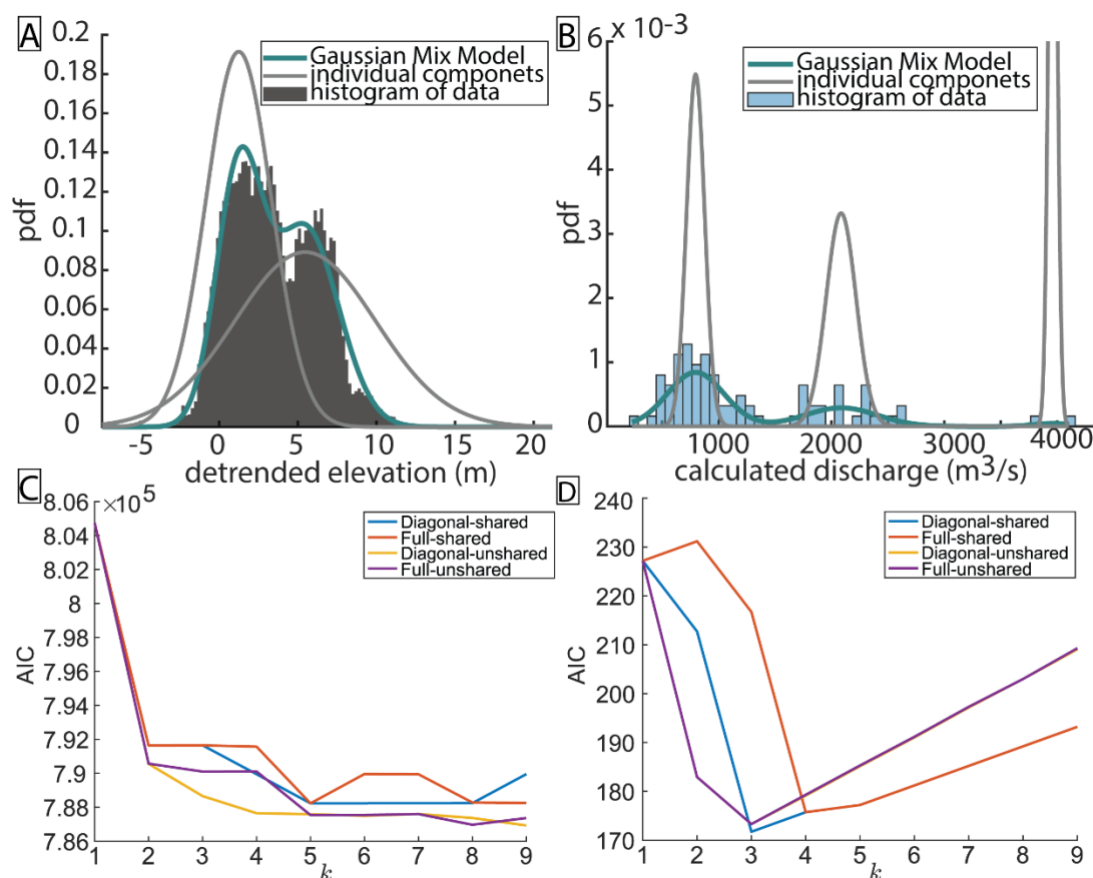


**Figure 9.** Mixing model fits to measured distributions of terrace elevation and estimated paleo-discharges. Distributions using elevation (A) and paleo-channels (B) support an interpretation of allogenic forcing for high terrace abandonment due to increasing decrease in discharge. Akaike Information Criterion (AIC) for detrended elevation (C) and paleo-discharge (D) mixing model. BIC results are not shown here but have similar trends to AIC. AIC results are shown for the mixing model that are solved for a diagonal and full covariance matrix and shared and unshared covariance. The model also used a small Regularization value to ensure the estimated covariance matrix is positive.

An important additional measurement used to assess whether terraces were abandoned due to enhanced local incision driven by gradient change during channel bend cut-off was the elevation differences between 40 adjacent terraces (**Fig. 10A**). These measured elevation differences between terraces were compared to estimated elevation changes produced by bend cut-offs. We used **Eq. 2** to calculate the elevation drop produced by a bend cutoff as:

$$\Delta \text{elevation}_{\text{bend cutoff}} = \text{length}_{\text{bend}} * \text{slope}_{\text{channel}} \quad (2)$$

Lengths of single paleo-channel bends were measured on several low, intermediate, and high Deweyville terraces using the bare-earth DEM (e.g. **Fig. 2**). The means and standard deviations for bend lengths on the low, intermediate and high terraces are  $5.7 \pm 2.8$  km ( $n = 3$ ),  $4.6 \pm 3.0$  km ( $n = 10$ ), and  $2.3 \pm 1.1$  km ( $n = 11$ ), respectively. We approximated channel slope using the planes fit to the terrace elevation points for each classification. The calculated mean slope and standard error for the low, intermediate, and high terraces are  $3.0 \times 10^{-4}$  ( $3.1 \times 10^{-6}$ ),  $2.9 \times 10^{-4}$  ( $1.1 \times 10^{-6}$ ), and  $3.0 \times 10^{-4}$  ( $1.2 \times 10^{-6}$ ), respectively. Using



Equation 2, estimated elevation drops driven by a possible bend cut-off are  $1.6 \pm 0.8$  m,  $1.3 \pm 0.9$  m, and  $0.7 \pm 0.3$  m (**Fig. 10A**).

An additional measurement used to evaluate the likelihood of terraces being produced by bend cut-off was the largest number of channel bends present in a segment of paleo-channel preserved on a terrace surface. Most terraces have one or fewer channel bends preserved (**Fig. 10B**) and only the intermediate and high Deweyville classifications possess terraces with more than two preserved channel bends.

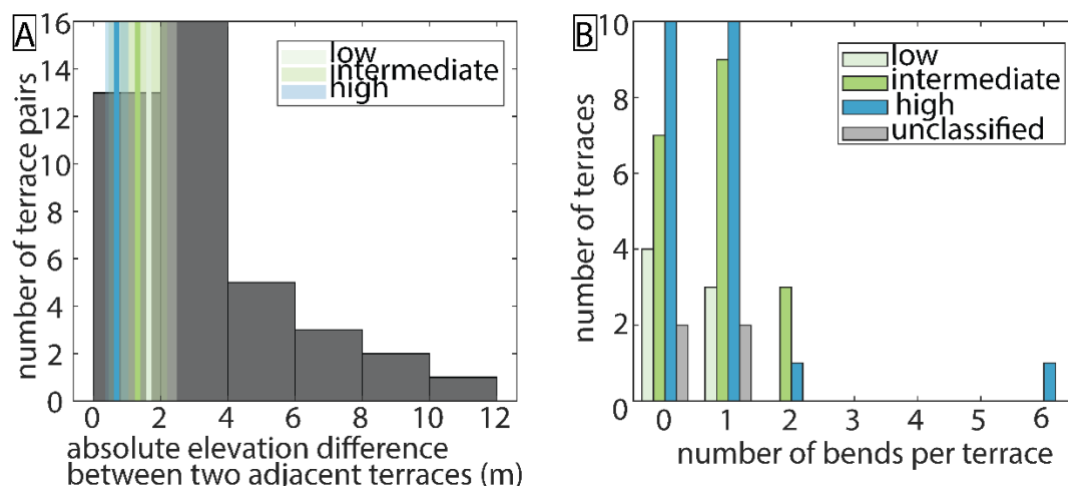


**Figure 10. Terrace properties used to assess the likelihood of meander bend-cutoff being the driver of terrace formation. (A)** Differences in elevation between adjacent terrace surfaces. Also plotted as vertical lines and swaths are the mean values  $\pm 1$  standard deviation for elevation decreases expected from cutting off a single meander bend for paleo-channels of the low, intermediate, and high Deweyville allogroups. **(B)** Maximum number of paleo-meander bends preserved in a channel segment on each terrace. Most terraces have between 0-1 channel bends preserved for one generation of channel. Only intermediate and high Deweyville terraces have more than two channel bends preserved by a paleo-channel.

## 4 Results

We mapped 52 terraces and 79 paleo-channel segments in the study area (**Fig. 1B**). Of these terraces, 22 are classified as high Deweyville, 19 as intermediate Deweyville, 8 as low Deweyville, and 4 were left unclassified as they could not be correlated with terraces mapped by either Blum et al. (1995) or Garvin (2008). Terraces vary in both size and shape, although they are typically elongate parallel to the valley axis and continuous for less than 10 km in that direction. The distribution of terraces is asymmetric, with more terraces observed on the east side of the valley (**Fig. 1B**). Consequently, most terraces are unpaired, meaning they have no topographic equivalent on the opposite side of the valley.

The best-fit planes to elevations for the Deweyville terrace groups defined by Blum et al. (1995), Garvin (2008), and Hidy et al. (2014) have RMSEs of 1.43m, 1.54m, and 1.41m for the low, intermediate, and high terraces respectively. Values of RMSE for best-fit planes to randomly grouped terraces are sensitive to the number of terraces defining a group. The smaller the number of terraces, the more likely it is that a low RMSE will result (**Fig. 6**). It is therefore important when comparing randomly grouped terraces to the officially classified groups that the number of terraces in each be the same. Running our





analysis of 50,000 sets of randomly assembled terraces with the same number of elements as the low ( $n=8$ ), intermediate ( $n=19$ ) and high ( $n=22$ ) Deweyville groups yielded the following RMSE results. The median and interquartile values of RMSE for planes fit to randomly selected terraces of the number present in the low-terrace classification are 1.82m, 1.55m, and 2.21m. The median and interquartile values of RMSE for planes fit to randomly selected terraces of the number present in the intermediate-terrace classification are 2.41m, 2.15m, and 2.66m. And finally, the median and interquartile values of RMSE for planes fit to randomly selected terraces of the number present in the high-terrace classification are 2.49m, 2.25m, and 2.71m.

The RMSE values for the best-fit planes to the classified Deweyville terraces are plotted on their associated synthetic RMSE distributions for randomly selected terraces in **Fig. 6**. Inspection of **Fig. 6** reveals little overlap between the classified high terraces and the random samplings of terraces. For the high Deweyville case, there was only a 0.008% occurrence of randomly selected terraces yielding an RMSE as low as 1.41m. A very different result was found for the classified low terraces, where its RMSE falls well within the associated distribution of synthetic RMSEs with fully 21% of all randomly selected cases having lower RMSE values. Minimal overlap was found between the RMSE for the classified intermediate terraces and the distribution of RMSE values generated from random terrace groupings. Only 1% of the randomly selected sets terraces were better fit to a plane than the classified group of intermediate terraces.

Mapped paleo-channels have widths that range from 82 to 543 m (**Fig. 7**). Estimated bankfull discharges calculated using these widths (**Eq. 1**) range from 233  $\text{m}^3/\text{s}$  to more than 4000  $\text{m}^3/\text{s}$  (**Fig. 8**). These paleo-discharges cluster into two groups, one at lower discharges centered around  $795 \pm 80 \text{ m}^3/\text{s}$  and one at higher discharges centered on  $2083 \pm 139 \text{ m}^3/\text{s}$  (**Fig. 9B**). The grouping of lower-discharge paleo-channels sit on terraces that have median elevations  $>4.5 \text{ m}$  above the modern valley floor and correspond to high Deweyville terraces (**Fig. 8**). The grouping of higher-discharge paleo-channels is preserved on terraces that have median elevations from 0.2 m below to 5.2 m above the modern floodplain and correspond to both intermediate and low Deweyville terraces (**Fig. 8**).

## 5 Discussion and Conclusions

Late Pleistocene terraces of the lower Trinity River valley formed during a period of net sea-level fall punctuated by shorter and smaller magnitude fluctuations (Anderson et al., 2016). Previous researchers have interpreted the formation of the Trinity terraces, as well as those observed in other Texas coastal valleys, in the context of these fluctuations (Blum et al., 1995; Morton et al., 1996; Rodriguez et al., 2005; Blum and Aslan, 2006). However, it has also been suggested that this terrace formation in the lower Trinity River valley was driven by autogenic triggers (Guerit et al., 2020). The motivation for this study was to develop tools to help distinguish between these two forcings that can produce terraces.

Several morphological characteristics exist to describe both the Trinity River terraces and their associated paleo-channels. The terraces are most commonly unpaired (**Fig. 1**), which is expected during autogenic terrace formation (Bull, 1990; Merritts et al., 1994; Finnegan and Dietrich, 2011; Limaye and Lamb, 2014, 2016). However, unpaired terraces can also be produced by unequal lateral river erosion that preferentially removes half of a previously formed pair of allogenic terraces



320 (Malatesta et al., 2017). The presence of unpaired terraces in the lower Trinity River valley may therefore be most indicative of the relative importance of lateral erosion for this system.

The number of channel bends preserved on terrace surfaces can be used as an indicator for autogenic versus allogenic processes. Allogenic terrace formation likely abandons larger terrace sections, preserving multiple channel bends. For incising rivers, the autogenic cut off of a single meander bend has been shown to be sufficient to produce the enhanced channel erosion  
 325 required to elevate relatively small sections of the previous active floodplain above flood levels (Limaye and Lamb, 2016; Finnegan and Dietrich, 2011). For the Trinity River, the observed elevation differences between adjacent terraces are similar to those predicted by cut off of a single meander bend (**Fig. 10A**). Many of the valley-ward edges of the lower and intermediate Deweyville Allogroups have the shapes of meander bends, recording the most outward extent of the active channel before the floodplain surface was abandoned (**Fig. 1, Fig. 2**). Furthermore, their tendency to be preserved as unpaired terraces with a  
 330 small number ( $< 2$ ) of channel bends is more consistent with the stochastic nature of meander cutoffs by autogenic processes than large-scale incisional events due to allogenic forcings (**Fig. 10A & 10B**, Finnegan and Dietrich, 2011; Limaye and Lamb, 2014, 2016). However, the morphology of the Trinity River valley terraces alone is not sufficient to distinguish between allogenic versus autogenic terrace formation.

We argue that a robust test for assessing the likelihood of autogenic versus allogenic forcing in terrace formation  
 335 comes from an analysis of the topographic variability of terrace sets inferred to have formed synchronously. Here we have developed a method to quantitatively compare elevation variability of any classified group of terraces against randomly selected terrace sets (**Fig. 5, Fig. 6**) so that we can evaluate whether a classified group is better organized than arbitrarily selected ones. For the lower Trinity River valley, if the Deweyville terraces formed synchronously (Blum et al., 1995; Morton et al., 1996; Rodriguez et al., 2005; Blum and Aslan, 2006), one would predict that terraces within these groups would show  
 340 lower variation about a best-fit plane than randomly grouped terraces (**Fig. 6**).

Our RMSE results show that the best-fit plane for the low Deweyville Allogroup cannot be separated from, and is instead consistent with, sets of randomly grouped terraces mimicking autogenic processes (**Fig. 6B**). The driver for the intermediate Deweyville Allogroup cannot be unambiguously determined based on the RMSE analysis. The classified group is better organized than most, but not all, randomly generated groupings of terraces (**Fig. 6C**). The overlap leads us to presume  
 345 that the null hypothesis of autogenic terrace formation cannot be robustly falsified. A different conclusion was reached for the high Deweyville Allogroup. With our RMSE analysis, we reject the null hypothesis of autogenic terrace formation. The high Deweyville Allogroup is most likely the product of punctuated allogenic change with an RMSE that is as small as any of the 50,000 values generated for random groupings of terraces (**Fig. 6A**). A difference between the low/intermediate versus high terraces was also found in the distribution of detrended terrace elevations using a 2 component Gaussian mixing model. The  
 350 first component of this model overlaps with elevations classified as low and intermediate Deweyville, while the second component corresponds most closely to high Deweyville elevations (**Fig. 4, Fig. 9A**). We, therefore, conclude that the high Deweyville terraces are different than the other two sets and record an allogenic signal connected with early valley incision.



The connections between potential discharge changes and terrace formation were assessed using paleo-channel widths and grain size (**Fig. 8, Fig. 9B**). Paleo-channel discharge estimates reveal a factor of two increase in bankfull discharge moving from older, high Deweyville terraces to younger, intermediate, and low Deweyville terraces. Recent synthesis studies by Phillip and Jerolmack (2016) and Dunne and Jerolmack (2018) confirm that these estimates of bankfull discharge are tied to moderate flooding and representative of mean climate properties. While our estimated discharge changes over time latest Pleistocene are large, it is only half of the proposed four times increase reported for similar paleo-channels preserved on terraces of the nearby lower Brazos River valley (Sylvia and Galloway, 2006).

Other river systems in the southeastern United States have the potential to also record a step-increase in formative discharge seen in the Trinity valley between the high to intermediate/low Deweyville terraces. This change was likely driven by a wetter climate in southeast Texas during the period ~34–20 ka, based on OSL dates for the low and intermediate Deweyville terraces (Garvin, 2008). During the Last Glacial Maximum (19–26 ka), precipitation in western and southwestern USA has been shown to be ~0.75–1.5 and ~1.3–1.6 of modern, respectively (Ibarra et al., 2018). Additionally, GCM models show a general increase in precipitation in the study area during the late Pleistocene (Roberts et al., 2014 (Fig. 2); McGee et al., 2018 (Fig. 2)). Our observations agree with other workers who interpreted the changes in channel size as an increase in mean discharge during this period (Saucier and Fleetwood, 1970; Alford and Holmes, 1985; Sylvia and Galloway, 2006; Gagliano and Thom, 1967). Observations of larger paleo-channels during this period are also seen across rivers in the southeast of Texas (e.g. Bernard, 1950; Blum et al., 1995; Sylvia and Galloway, 2006), Arkansas and Louisiana (e.g. Saucier and Fleetwood, 1970), and Georgia and South Carolina (e.g. Leigh and Feeney, 1995; Leigh et al., 2004; Leigh, 2008).

The estimated changes through time in bankfull discharge are not matched by estimated changes in river long-profile or paleo-slope. Previously discussed best-fit planes to the Deweyville Allogroups have slopes that are roughly constant and indistinguishable from the modern long profile for the Trinity River. Theory by Parker et al. (1998) and experiments by Whipple et al., (1998) have demonstrated long-profile slope for sandy fluvial systems is a function of sediment-to-water discharges. Maintenance of a roughly constant slope while water discharge changed therefore almost certainly required commensurate changes to sediment discharge. Responsive adjustments to sediment discharge suggest that throughout the latest Pleistocene, the river itself remained a predominantly transport limited system (Whipple, 2002; Howard, 1980).

We have shown that a majority of Deweyville terraces in the Trinity valley preserve no more than a single paleo-channel bend (**Fig. 10B**) and that elevation differences between adjacent terraces are similar to an expected elevation change driven by channel shortening through cut off to a river bend (**Fig. 10A**). These terrace properties highlight an opportunity for our community to measure the number of bends involved in the autogenic shortening of river channels. Specifically, there is an opportunity to quantify what percentage of cutoffs result in two or more bends being detached from the active channel in short amounts of time, thereby refining an expected upper limit to the number of channel bends preserved on autogenically generated terraces. An additional mechanism for reducing uncertainty in the processes that cut Trinity terraces would be assembling a greater number of terrace ages. Increasing age control could constrain vertical versus lateral migration rates for



the river to a point where autogenic versus allogenic processes connected to terrace formation are separable (Limaye and Lamb, 2016; Merritts et al., 1994).

390 The results presented here demonstrate that it is critical to understand the many potential forcings (both allogenic and autogenic) on a river system that can lead to terrace formation and to employ robust, quantitative tests for discriminating between these forcings before using terraces to reconstruct paleo environmental histories. The method proposed here for assessing the role of allogenic processes in terrace formation using the variability of terrace elevations provides a simple, quantitative test, may prove useful for interpreting terrace formation in other river systems.

### Data availability

395 The lidar dataset was acquired from the Texas Natural Resource Information System (TNRIS) at <https://tnris.org>. Please see the reference to each dataset. Tables with analysis produced from the lidar datasets are included in the supplementary material.

### Author contribution

All authors designed the analysis and contributed to the manuscript writing. HHG and TE analyzed the lidar dataset. TG developed the code to fit planes to the lidar dataset.

### Competing interests

400 The authors declare that they have no conflict of interest.

### Acknowledgments

405 We thank Webster Mangham for providing the report from the Trinity River Authority of Texas Phase II, Bathymetry and Sediment Collection for the Port of Liberty Study. We also thank Joel Johnson, Gary Kocurek, and Ajay Limaye for insightful comments on early versions of the manuscript as well as Niels Hovius, Mike Lamb, Paola Passalacqua, and Daniella Rempe for additional comments. HHG was funded by the Jackson School of Geoscience Recruiting Fellowship and the National Science Foundation Graduate Research Fellowship.

### References

- Alford, J. J. and Holmes, J. C.: Meander Scars as Evidence of Major Climate Change in Southwest Louisiana, *Ann. Assoc. Am. Geogr.*, 75, 395–403, <https://doi.org/10.1111/j.1467-8306.1985.tb00074.x>, 1985.
- 410 Anderson, J. B., Wallace, D. J., Simms, A. R., Rodriguez, A. B., and Milliken, K. T.: Variable response of coastal environments



- of the northwestern Gulf of Mexico to sea-level rise and climate change: Implications for future change, *Mar. Geol.*, 352, 348–366, <https://doi.org/10.1016/j.margeo.2013.12.008>, 2014.
- Anderson, J. B., Wallace, D. J., Simms, A. R., Rodriguez, A. B., Weight, R. W. R., and Taha, Z. P.: Recycling sediments between source and sink during a eustatic cycle: Systems of late Quaternary northwestern Gulf of Mexico Basin, *Earth-Science Rev.*, 153, 111–138, <https://doi.org/10.1016/j.earscirev.2015.10.014>, 2016.
- 415 Baker, E. T. J.: Stratigraphic Nomenclature and Geologic Sections of the Gulf, U.S. Geol. Surv. Open-File Rep., 94–461, 34, 1995.
- Bernard, H. A.: Quaternary Geology of Southeast Texas, LSU Historical Dissertations and Theses 7952, [https://doi.org/https://digitalcommons.lsu.edu/gradschool\\_disstheses/7952](https://doi.org/https://digitalcommons.lsu.edu/gradschool_disstheses/7952), 1950.
- 420 Blum, M., Martin, J., Milliken, K., and Garvin, M.: Paleovalley systems: Insights from Quaternary analogs and experiments, *Earth-Science Rev.*, 116, 128–169, <https://doi.org/10.1016/j.earscirev.2012.09.003>, 2013.
- Blum, M. D. and Aslan, A.: Signatures of climate vs. sea-level change within incised valley-fill successions: Quaternary examples from the Texas GULF Coast, *Sediment. Geol.*, 190, 177–211, <https://doi.org/10.1016/j.sedgeo.2006.05.024>, 2006.
- Blum, M. D. and Törnqvist, T. E.: Fluvial responses to climate and sea-level change: A review and look forward, 425 *Sedimentology*, 47, 2–48, <https://doi.org/10.1046/j.1365-3091.2000.00008.x>, 2000.
- Blum, M. D., Morton, R. A., and Durbin, J. M.: “Deweyville” Terraces and Deposits of the Texas Gulf Coastal Plain, *GCAGS Trans.*, 45, 53–60, 1995.
- Bull, W. B.: Stream-terrace genesis: implications for soil development, 3, 351–367, [https://doi.org/10.1016/0169-555X\(90\)90011-E](https://doi.org/10.1016/0169-555X(90)90011-E), 1990.
- 430 Church, M.: Bed Material Transport and the Morphology of Alluvial River Channels, *Annu. Rev. Earth Planet. Sci.*, 34, 325–354, <https://doi.org/10.1146/annurev.earth.33.092203.122721>, 2006.
- Daley, J. and Cohen, T.: Climatically-Controlled River Terraces in Eastern Australia, 1, 23, <https://doi.org/10.3390/quat1030023>, 2018.
- FEMA: FEMA 2011 1m Liberty Lidar, 2011.
- 435 Finnegan, N. J. and Dietrich, W. E.: Episodic bedrock strath terrace formation due to meander migration and cutoff, *Geology*, 39, 143–146, <https://doi.org/10.1130/G31716.1>, 2011.
- Gagliano, S. M. and Thom, B. G.: Deweyville Terrace, Gulf and Atlantic Coasts. Technical Report 39., Baton Rouge, 23–41 pp., 1967.
- Galloway, W. E., Ganey-Curry, P. E., Li, X., and Buffler, R. T.: Cenozoic depositional history of the Gulf of Mexico basin, 440 *Am. Assoc. Pet. Geol. Bull.*, 84, 1743–1774, <https://doi.org/10.1306/8626C37F-173B-11D7-8645000102C1865D>, 2000.
- Garvin, M. G.: Late Quaternary geochronologic, stratigraphic, and sedimentologic framework of the Trinity River incised valley: East Texas coast, 2008.
- Guerit, L., Foreman, B. Z., Chen, C., Paola, C., and Castelltort, S.: Autogenic delta progradation during sea-level rise within incised valleys, *Geology*, XX, 1–5, <https://doi.org/10.1130/g47976.1>, 2020.



- 445 Hancock, G. S. and Anderson, R. S.: Numerical modelling of fluvial strath terrace formation in response to oscillating climate, *Geol. Soc. Am. Bull.*, 114, 1131–1142, [https://doi.org/10.1130/0016-7606\(2002\)114<1131, 2002](https://doi.org/10.1130/0016-7606(2002)114<1131, 2002).
- Heinrich, P., Miner, M., Paulsell, R., and McCulloh, R.: Response of Late Quaternary Valley systems to Holocene sea level rise on continental shelf offshore Louisiana: preservation potential of paleolandscapes, 2020.
- Hidy, A. J., Gosse, J. C., Blum, M. D., and Gibling, M. R.: Glacial-interglacial variation in denudation rates from interior  
 450 Texas, USA, established with cosmogenic nuclides, *Earth Planet. Sci. Lett.*, 390, 209–221, <https://doi.org/10.1016/j.epsl.2014.01.011>, 2014.
- Howard, A. D.: Thresholds in river regimes, in: *Thresholds in geomorphology*, 227–258, 1980.
- Ibarra, D. E., Oster, J. L., Winnick, M. J., Rugenstein, J. K. C., Byrne, M. P., and Chamberlain, C. P.: Warm and cold wet states in the western United States during the Pliocene-Pleistocene, *Geology*, 46, 355–358, <https://doi.org/10.1130/G39962.1>,  
 455 2018.
- Knox, J. C.: Responses of floods to Holocene climatic change in the upper Mississippi Valley, *Quat. Res.*, 23, 287–300, [https://doi.org/10.1016/0033-5894\(85\)90036-5](https://doi.org/10.1016/0033-5894(85)90036-5), 1985.
- Leigh, D. S.: Late Quaternary climates and river channels of the Atlantic Coastal Plain, Southeastern USA, 101, 90–108, <https://doi.org/10.1016/j.geomorph.2008.05.024>, 2008.
- 460 Leigh, D. S. and Feeney, T. P.: Paleochannels indicating wet climate and lack of response to lower sea level, southeast Georgia, *Geology*, 23, 687–690, [https://doi.org/10.1130/0091-7613\(1995\)023<0687:PIWCAL>2.3.CO;2](https://doi.org/10.1130/0091-7613(1995)023<0687:PIWCAL>2.3.CO;2), 1995.
- Leigh, D. S., Srivastava, P., and Brook, G. A.: Late Pleistocene braided rivers of the Atlantic Coastal Plain, USA, *Quat. Sci. Rev.*, 23, 65–84, [https://doi.org/10.1016/S0277-3791\(03\)00221-X](https://doi.org/10.1016/S0277-3791(03)00221-X), 2004.
- Limaye, A. B. S. and Lamb, M. P.: Numerical simulations of bedrock valley evolution by meandering rivers with variable  
 465 bank material, *J. Geophys. Res. Earth Surf.*, 119, 927–950, <https://doi.org/10.1002/2013JF002997>, 2014.
- Limaye, A. B. S. and Lamb, M. P.: Numerical model predictions of autogenic fluvial terraces and comparison to climate change expectations, *J. Geophys. Res. Earth Surf.*, n/a-n/a, <https://doi.org/10.1002/2014JF003392>, 2016.
- Malatesta, L. C., Prancevic, J. P., and Avouac, J. P.: Autogenic entrenchment patterns and terraces due to coupling with lateral erosion in incising alluvial channels, *J. Geophys. Res. Earth Surf.*, 122, 335–355, <https://doi.org/10.1002/2015JF003797>, 2017.
- 470 McGee, D., Moreno-Chamarro, E., Marshall, J., and Galbraith, E. D.: Western U.S. lake expansions during Heinrich stadials linked to Pacific Hadley circulation, *Sci. Adv.*, 4, 1–11, <https://doi.org/10.1126/sciadv.aav0118>, 2018.
- Merritts, D. J., Vincent, K. R., and Wohl, E. E.: Long river profiles, tectonism, and eustasy: A guide to interpreting fluvial terraces, *J. Geophys. Res. Solid Earth*, 99, 14031–14050, <https://doi.org/10.1029/94JB00857>, 1994.
- Molnar, P., Brown, E. T., Burchfiel, B. C., Deng, Q., Feng, X., Li, J., Raisbeck, G. M., Shi, J., Zhangming, W., Yiou, F., and  
 475 You, H.: Quaternary Climate Change and the Formation of River Terraces across Growing Anticlines on the North Flank of the Tien Shan, China, *J. Geol.*, 102, 583–602, <https://doi.org/10.1086/629700>, 1994.
- Morton, R. A., Blum, M. D., and White, W. A.: Valley Fills of Incised Coastal Plain Rivers, Southeastern Texas, Gulf Coast Assoc. Geol. Soc., 46, 321–331, <https://doi.org/10.1306/2DC40B2D-0E47-11D7-8643000102C1865D>, 1996.





- Muto, T. and Steel, R. J.: Autogenic response of fluvial deltas to steady sea-level fall: Implications from flume-tank  
 480 experiments, *Geology*, 32, 401–404, <https://doi.org/10.1130/G20269.1>, 2004.
- Parker, G., Paola, C., Whipple, K. X., and Mohrig, D.: Alluvial Fans Formed by Channelized Fluvial and Sheet Flow. I: Theory, *J. Hydraul. Eng.*, 124, 985–995, [https://doi.org/10.1061/\(ASCE\)0733-9429\(1998\)124:10\(985\)](https://doi.org/10.1061/(ASCE)0733-9429(1998)124:10(985)), 1998.
- Pazzaglia, F. J.: Fluvial Terraces, in: *Treatise on Geomorphology*, vol. 9, 379–412, <https://doi.org/10.1016/B978-0-12-374739-6.00248-7>, 2013.
- 485 Pazzaglia, F. J. and Gardner, T. W.: Fluvial terraces of the lower Susquehanna River, 8, 83–113, [https://doi.org/10.1016/0169-555X\(93\)90031-V](https://doi.org/10.1016/0169-555X(93)90031-V), 1993.
- Pazzaglia, F. J., Gardner, T. W., and Merritts, D. J.: Bedrock fluvial incision and longitudinal profile development over geologic time scales determined by fluvial terraces, 207–235, <https://doi.org/10.1029/GM107p0207>, 1998.
- Roberts, W. H. G., Valdes, P. J., and Payne, A. J.: Topography’s crucial role in Heinrich Events, *Proc. Natl. Acad. Sci. U. S.*  
 490 *A.*, 111, 16688–16693, <https://doi.org/10.1073/pnas.1414882111>, 2014.
- Rodriguez, A. B., Anderson, J. B., and Simms, A. R.: Terrace Inundation as an Autocyclic Mechanism for Parasequence Formation: Galveston Estuary, Texas, U.S.A., *J. Sediment. Res.*, 75, 608–620, <https://doi.org/10.2110/jsr.2005.050>, 2005.
- Saucier, R. T.: *Geomorphology and Quaternary Geologic History of the Lower Mississippi Valley*, US Army Corps Eng., I, 1–414, 1994.
- 495 Saucier, R. T. and Fleetwood, A. R.: Origin and Chronologic Significance of Late Quaternary Terraces, Ouachita River, Arkansas and Louisiana, *GSA Bull.*, 81, 869–890, [https://doi.org/10.1130/0016-7606\(1970\)81\[869:OACSOL\]2.0.CO;2](https://doi.org/10.1130/0016-7606(1970)81[869:OACSOL]2.0.CO;2), 1970.
- Simms, A. R., Anderson, J. B., Milliken, K. T., Taha, Z. P., and Wellner, J. S.: Geomorphology and age of the oxygen isotope stage 2 (last lowstand) sequence boundary on the northwestern Gulf of Mexico continental shelf, *Geol. Soc. Spec. Publ.*, 277, 29–46, <https://doi.org/10.1144/GSL.SP.2007.277.01.03>, 2007.
- 500 Smith, V. B. and Mohrig, D.: Geomorphic signature of a dammed Sandy River: The lower Trinity River downstream of Livingston Dam in Texas, USA, 297, 122–136, <https://doi.org/10.1016/j.geomorph.2017.09.015>, 2017.
- Strong, N. and Paola, C.: Fluvial Landscapes and Stratigraphy in a Flume, *Sediment. Rec.*, 4, 4–8, <https://doi.org/10.2110/sedred.2006.2.4>, 2006.
- Sylvia, D. A. and Galloway, W. E.: Morphology and stratigraphy of the late Quaternary lower Brazos valley: Implications for  
 505 paleo-climate, discharge and sediment delivery, *Sediment. Geol.*, 190, 159–175, <https://doi.org/10.1016/j.sedgeo.2006.05.023>, 2006.
- Thomas, M. A. and Anderson, J. B.: Sea-Level Controls on the Facies Architecture of the Trinity/Sabine Incised-Valley System, Texas Continental Shelf, in: *Incised-Valley Systems: Origin and Sedimentary Sequences.*, SEPM Society for Sedimentary Geology, <https://doi.org/10.2110/pec.94.12.0063>, 1994.
- 510 Trinity River Authority of Texas: Phase II, Bathymetry and Sediment Collection for Port of Liberty Study, 2017.
- National Water Information System data available on the World Wide Web (USGS Water Data for the Nation),: <https://waterdata.usgs.gov/usa/nwis/uv?08066500>.



National Water Information System data available on the World Wide Web (USGS Water Data for the Nation):  
[https://waterdata.usgs.gov/nwis/uv?site\\_no=08067000](https://waterdata.usgs.gov/nwis/uv?site_no=08067000).

- 515 Wegmann, K. W. and Pazzaglia, F. J.: Holocene strath terraces, climate change, and active tectonics: The Clearwater River basin, Olympic Peninsula, Washington State, *Bull. Geol. Soc. Am.*, 114, 731–744, [https://doi.org/10.1130/0016-7606\(2002\)114<0731:HSTCCA>2.0.CO;2](https://doi.org/10.1130/0016-7606(2002)114<0731:HSTCCA>2.0.CO;2), 2002.

Whipple, K. X.: Implications of sediment-flux-dependent river incision models for landscape evolution, *J. Geophys. Res.*, 107, 2039, <https://doi.org/10.1029/2000JB000044>, 2002.

- 520 Whipple, K. X., Parker, G., Paola, C., and Mohrig, D.: Channel Dynamics, Sediment Transport, and the Slope of Alluvial Fans: Experimental Study, *J. Geol.*, 106, 677–694, <https://doi.org/10.1086/516053>, 1998.

Wilkerson, G. V. and Parker, G.: Physical Basis for Quasi-Universal Relationships Describing Bankfull Hydraulic Geometry of Sand-Bed Rivers, *J. Hydraul. Eng.*, 137, 739–753, [https://doi.org/10.1061/\(ASCE\)HY.1943-7900.0000352](https://doi.org/10.1061/(ASCE)HY.1943-7900.0000352), 2011.

- 525 Young, S. C., Ewing, T., Hamlin, S., Baker, E., and Lupton, D.: Final Report Updating the Hydrogeologic Framework for the Northern Portion of the Gulf Coast Aquifer, 2012.